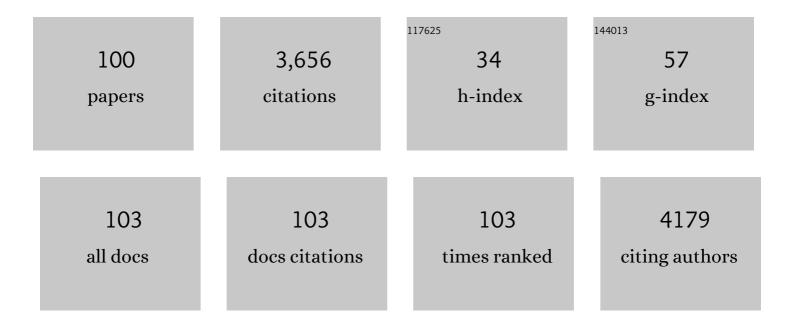
Michael L Neidig

List of Publications by Year in descending order

Source: https://exaly.com/author-pdf/3496800/publications.pdf Version: 2024-02-01



MICHAEL | NEIDIC

#	Article	IF	CITATIONS
1	Covalency in f-element complexes. Coordination Chemistry Reviews, 2013, 257, 394-406.	18.8	415
2	Spectroscopic and electronic structure studies of aromatic electrophilic attack and hydrogen-atom abstraction by non-heme iron enzymes. Proceedings of the National Academy of Sciences of the United States of America, 2006, 103, 12966-12973.	7.1	143
3	A Combined Mössbauer, Magnetic Circular Dichroism, and Density Functional Theory Approach for Iron Cross-Coupling Catalysis: Electronic Structure, In Situ Formation, and Reactivity of Iron-Mesityl-Bisphosphines. Journal of the American Chemical Society, 2014, 136, 9132-9143.	13.7	108
4	VTVH-MCD and DFT Studies of Thiolate Bonding to {FeNO}7/{FeO2}8Complexes of IsopenicillinNSynthase:Â Substrate Determination of Oxidase versus Oxygenase Activity in Nonheme Fe Enzymes. Journal of the American Chemical Society, 2007, 129, 7427-7438.	13.7	105
5	Iron(II) Active Species in Iron–Bisphosphine Catalyzed Kumada and Suzuki–Miyaura Cross-Couplings of Phenyl Nucleophiles and Secondary Alkyl Halides. Journal of the American Chemical Society, 2015, 137, 11432-11444.	13.7	101
6	Mechanism of the Decomposition of Aqueous Hydrogen Peroxide over Heterogeneous TiSBA15 and TS-1 Selective Oxidation Catalysts: Insights from Spectroscopic and Density Functional Theory Studies. ACS Catalysis, 2011, 1, 1665-1678.	11.2	99
7	Catalytic Light-Driven Generation of Hydrogen from Water by Iron Dithiolene Complexes. Journal of the American Chemical Society, 2016, 138, 11654-11663.	13.7	96
8	Development and Evolution of Mechanistic Understanding in Iron-Catalyzed Cross-Coupling. Accounts of Chemical Research, 2019, 52, 140-150.	15.6	92
9	Structure–function correlations in oxygen activating non-heme iron enzymes. Chemical Communications, 2005, , 5843.	4.1	90
10	Iron Phosphine Catalyzed Cross-Coupling of Tetraorganoborates and Related Group 13 Nucleophiles with Alkyl Halides. Organometallics, 2014, 33, 5767-5780.	2.3	90
11	Formation and Stabilization of Fluorescent Gold Nanoclusters Using Small Molecules. Journal of Physical Chemistry C, 2010, 114, 15879-15882.	3.1	88
12	CD and MCD of CytC3 and Taurine Dioxygenase:  Role of the Facial Triad in α-KG-Dependent Oxygenases. Journal of the American Chemical Society, 2007, 129, 14224-14231.	13.7	86
13	Isolation, Characterization, and Reactivity of Fe ₈ Me ₁₂ [–] : Kochi's <i>S</i> = 1/2 Species in Iron-Catalyzed Cross-Couplings with MeMgBr and Ferric Salts. Journal of the American Chemical Society, 2016, 138, 7492-7495.	13.7	81
14	Intermediates and Mechanism in Iron-Catalyzed Cross-Coupling. Journal of the American Chemical Society, 2018, 140, 11872-11883.	13.7	79
15	Ag K-Edge EXAFS Analysis of DNA-Templated Fluorescent Silver Nanoclusters: Insight into the Structural Origins of Emission Tuning by DNA Sequence Variations. Journal of the American Chemical Society, 2011, 133, 11837-11839.	13.7	78
16	How Innocent are Potentially Redox Non-Innocent Ligands? Electronic Structure and Metal Oxidation States in Iron-PNN Complexes as a Representative Case Study. Inorganic Chemistry, 2015, 54, 4909-4926.	4.0	76
17	A Combined Probe-Molecule, Mössbauer, Nuclear Resonance Vibrational Spectroscopy, and Density Functional Theory Approach for Evaluation of Potential Iron Active Sites in an Oxygen Reduction Reaction Catalyst. Journal of Physical Chemistry C, 2017, 121, 16283-16290.	3.1	75
18	Activation of α-Keto Acid-Dependent Dioxygenases: Application of an {FeNO} ⁷ /{FeO ₂ } ⁸ Methodology for Characterizing the Initial Steps of O ₂ Activation. Journal of the American Chemical Society, 2011, 133, 18148-18160.	13.7	66

#	Article	IF	CITATIONS
19	The <i>N</i> â€Methylpyrrolidone (NMP) Effect in Ironâ€Catalyzed Crossâ€Coupling with Simple Ferric Salts and MeMgBr. Angewandte Chemie - International Edition, 2018, 57, 6496-6500.	13.8	64
20	Isolation and Characterization of a Tetramethyliron(III) Ferrate: An Intermediate in the Reduction Pathway of Ferric Salts with MeMgBr. Journal of the American Chemical Society, 2014, 136, 15457-15460.	13.7	61
21	CD and MCD Studies of the Non-Heme Ferrous Active Site in (4-Hydroxyphenyl)pyruvate Dioxygenase:Â Correlation between Oxygen Activation in the Extradiol and α-KG-Dependent Dioxygenases. Journal of the American Chemical Society, 2004, 126, 4486-4487.	13.7	60
22	Iron Dicarbonyl Complexes Featuring Bipyridineâ€Based PNN Pincer Ligands with Short Interpyridine CC Bond Lengths: Innocent or Nonâ€Innocent Ligand?. Chemistry - A European Journal, 2014, 20, 4403-4413.	3.3	56
23	General method for iron-catalyzed multicomponent radical cascades–cross-couplings. Science, 2021, 374, 432-439.	12.6	53
24	Terminal coordination of diatomic boron monofluoride to iron. Science, 2019, 363, 1203-1205.	12.6	50
25	Spectroscopic Characterization of Soybean Lipoxygenase-1 Mutants:  the Role of Second Coordination Sphere Residues in the Regulation of Enzyme Activity. Biochemistry, 2003, 42, 7294-7302.	2.5	49
26	Polyoxovanadate–Alkoxide Clusters as a Redox Reservoir for Iron. Inorganic Chemistry, 2017, 56, 7065-7080.	4.0	48
27	Facile hydrogen atom transfer to iron(<scp>iii</scp>) imido radical complexes supported by a dianionic pentadentate ligand. Chemical Science, 2016, 7, 5939-5944.	7.4	47
28	Intermediates and Reactivity in Iron-Catalyzed Cross-Couplings of Alkynyl Grignards with Alkyl Halides. Journal of the American Chemical Society, 2017, 139, 6988-7003.	13.7	46
29	The Three-His Triad in Dke1: Comparisons to the Classical Facial Triad. Biochemistry, 2010, 49, 6945-6952.	2.5	44
30	A combined magnetic circular dichroism and density functional theory approach for the elucidation of electronic structure and bonding in three- and four-coordinate iron(<scp>ii</scp>)–N-heterocyclic carbene complexes. Chemical Science, 2015, 6, 1178-1188.	7.4	44
31	Insight into contributions to phenol selectivity in the solution oxidation of benzene to phenol with H2O2. Catalysis Communications, 2011, 12, 480-484.	3.3	41
32	The Effect of βâ€Hydrogen Atoms on Iron Speciation in Crossâ€Couplings with Simple Iron Salts and Alkyl Grignard Reagents. Angewandte Chemie - International Edition, 2019, 58, 2769-2773.	13.8	41
33	Identification and Reactivity of Cyclometalated Iron(II) Intermediates in Triazole-Directed Iron-Catalyzed C–H Activation. Journal of the American Chemical Society, 2019, 141, 12338-12345.	13.7	39
34	Linear and T-Shaped Iron(I) Complexes Supported by N-Heterocyclic Carbene Ligands: Synthesis and Structure Characterization. Inorganic Chemistry, 2015, 54, 8808-8816.	4.0	36
35	Multinuclear iron–phenyl species in reactions of simple iron salts with PhMgBr: identification of Fe4(μ-Ph)6(THF)4 as a key reactive species for cross-coupling catalysis. Chemical Science, 2018, 9, 7931-7939.	7.4	34
36	Flexible Binding of PNP Pincer Ligands to Monomeric Iron Complexes. Inorganic Chemistry, 2014, 53, 6066-6072.	4.0	32

#	Article	IF	CITATIONS
37	Electronic Structure and Bonding in Iron(II) and Iron(I) Complexes Bearing Bisphosphine Ligands of Relevance to Iron-Catalyzed C–C Cross-Coupling. Inorganic Chemistry, 2016, 55, 272-282.	4.0	32
38	Two- and three-coordinate formal iron(<scp>i</scp>) compounds featuring monodentate aminocarbene ligands. Organic Chemistry Frontiers, 2014, 1, 1040-1044.	4.5	31
39	Manipulating Magneto-Optic Properties of a Chiral Polymer by Doping with Stable Organic Biradicals. Nano Letters, 2016, 16, 5451-5455.	9.1	30
40	Mechanism of the Bis(imino)pyridine-Iron-Catalyzed Hydromagnesiation of Styrene Derivatives. Journal of the American Chemical Society, 2019, 141, 10099-10108.	13.7	30
41	Spectroscopic and computational studies of NTBC bound to the non-heme iron enzyme (4-hydroxyphenyl)pyruvate dioxygenase: Active site contributions to drug inhibition. Biochemical and Biophysical Research Communications, 2005, 338, 206-214.	2.1	28
42	NHC and nucleophile chelation effects on reactive iron(ii) species in alkyl–alkyl cross-coupling. Chemical Science, 2018, 9, 1878-1891.	7.4	28
43	Kinetic and Spectroscopic Studies of N694C Lipoxygenase:  A Probe of the Substrate Activation Mechanism of a Nonheme Ferric Enzyme. Journal of the American Chemical Society, 2007, 129, 7531-7537.	13.7	27
44	Atom-Economical Ni-Catalyzed Diborylative Cyclization of Enynes: Preparation of Unsymmetrical Diboronates. Organic Letters, 2019, 21, 6552-6556.	4.6	26
45	Reactivity of (NHC) ₂ FeX ₂ Complexes toward Arylborane Lewis Acids and Arylboronates. Organometallics, 2014, 33, 370-377.	2.3	25
46	A Physicalâ€Inorganic Approach for the Elucidation of Active Iron Species and Mechanism in Ironâ€Catalyzed Crossâ€Coupling. Israel Journal of Chemistry, 2017, 57, 1106-1116.	2.3	24
47	Homoleptic Aryl Complexes of Uranium (IV). Angewandte Chemie - International Edition, 2019, 58, 10266-10270.	13.8	24
48	Mononuclear, Dinuclear, and Trinuclear Iron Complexes Featuring a New Monoanionic SNS Thiolate Ligand. Inorganic Chemistry, 2016, 55, 987-997.	4.0	23
49	Iron(II) Complexes of a Hemilabile SNS Amido Ligand: Synthesis, Characterization, and Reactivity. Inorganic Chemistry, 2017, 56, 13766-13776.	4.0	22
50	Magnetic circular dichroism studies of iron(<scp>ii</scp>) binding to human calprotectin. Chemical Science, 2017, 8, 1369-1377.	7.4	22
51	Additive and Counterion Effects in Iron-Catalyzed Reactions Relevant to C–C Bond Formation. ACS Catalysis, 2021, 11, 8493-8503.	11.2	22
52	Magnetic circular dichroism of UCl ₆ ^{â^'} in the ligand-to-metal charge-transfer spectral region. Physical Chemistry Chemical Physics, 2017, 19, 17300-17313.	2.8	21
53	Activation of ammonia and hydrazine by electron rich Fe(<scp>ii</scp>) complexes supported by a dianionic pentadentate ligand platform through a common terminal Fe(<scp>iii</scp>) amido intermediate. Chemical Science, 2021, 12, 2231-2241.	7.4	21
54	Efficient Nazarov Cyclization/Wagner–Meerwein Rearrangement Terminated by a Cu ^{II} â€Promoted Oxidation: Synthesis of 4â€Alkylidene Cyclopentenones. Chemistry - A European Journal, 2013, 19, 4842-4848.	3.3	20

#	Article	IF	CITATIONS
55	The <i>N</i> â€Methylpyrrolidone (NMP) Effect in Ironâ€Catalyzed Crossâ€Coupling with Simple Ferric Salts and MeMgBr. Angewandte Chemie, 2018, 130, 6606-6610.	2.0	19
56	Magnetic circular dichroism and density functional theory studies of electronic structure and bonding in cobalt(ii)–N-heterocyclic carbene complexes. Dalton Transactions, 2017, 46, 13290-13299.	3.3	18
57	Kinetic, Spectroscopic, and Structural Investigations of the Soybean Lipoxygenase-1 First-Coordination Sphere Mutant, Asn694Glyâ€,‡. Biochemistry, 2006, 45, 10233-10242.	2.5	17
58	Direct Observation of Acetyl Group Formation from the Reaction of CO with Methylated H-MOR by in Situ Diffuse Reflectance Infrared Spectroscopy. Journal of Physical Chemistry Letters, 2010, 1, 3012-3015.	4.6	17
59	Spectroscopic and electronic structure studies of the role of active site interactions in the decarboxylation reaction of α-keto acid-dependent dioxygenases. Journal of Inorganic Biochemistry, 2006, 100, 2108-2116.	3.5	16
60	Combined Effects of Backbone and N-Substituents on Structure, Bonding, and Reactivity of Alkylated Iron(II)-NHCs. Organometallics, 2018, 37, 3093-3101.	2.3	16
61	A Pseudotetrahedral Uranium(V) Complex. Inorganic Chemistry, 2018, 57, 8106-8115.	4.0	16
62	Backbone Dehydrogenation in Pyrrole-Based Pincer Ligands. Inorganic Chemistry, 2018, 57, 9544-9553.	4.0	16
63	Insight into the Electronic Structure of Formal Lanthanide(II) Complexes using Magnetic Circular Dichroism Spectroscopy. Organometallics, 2019, 38, 3124-3131.	2.3	16
64	The Effect of βâ€Hydrogen Atoms on Iron Speciation in Crossâ€Couplings with Simple Iron Salts and Alkyl Grignard Reagents. Angewandte Chemie, 2019, 131, 2795-2799.	2.0	16
65	The Exceptional Diversity of Homoleptic Uranium–Methyl Complexes. Angewandte Chemie - International Edition, 2020, 59, 13586-13590.	13.8	16
66	Ambivalent binding between a radical-based pincer ligand and iron. Dalton Transactions, 2015, 44, 10516-10523.	3.3	15
67	Magnetic Circular Dichroism and Density Functional Theory Studies of Iron(II)-Pincer Complexes: Insight into Electronic Structure and Bonding Effects of Pincer N-Heterocyclic Carbene Moieties. Organometallics, 2016, 35, 3692-3700.	2.3	14
68	TMEDA in Ironâ€Catalyzed Hydromagnesiation: Formation of Iron(II)â€Alkyl Species for Controlled Reduction to Alkene‧tabilized Iron(0). Angewandte Chemie - International Edition, 2020, 59, 17070-17076.	13.8	14
69	Possible Demonstration of a Polaronic Bose-Einstein(-Mott) Condensate in UO2(+x) by Ultrafast THz Spectroscopy and Microwave Dissipation. Scientific Reports, 2015, 5, 15278.	3.3	13
70	Transition-Metal-Free Formation of C–E Bonds (E = C, N, O, S) and Formation of C–M Bonds (M = Mn,) Tj ET Organometallics, 2017, 36, 849-857.	Qq0 0 0 rş 2.3	gBT /Overlock 12
71	Ligand effects on electronic structure and bonding in U(<scp>iii</scp>) coordination complexes: a combined MCD, EPR and computational study. Dalton Transactions, 2020, 49, 14401-14410.	3.3	12
72	[2Fe–2S] Cluster Supported by Redox-Active <i>o</i> -Phenylenediamide Ligands and Its Application	4.0	12

toward Dinitrogen Reduction. Inorganic Chemistry, 2021, 60, 13811-13820.

#	Article	IF	CITATIONS
73	Creation of an unexpected plane of enhanced covalency in cerium(III) and berkelium(III) terpyridyl complexes. Nature Communications, 2021, 12, 7230.	12.8	11
74	<i>C</i> -Term magnetic circular dichroism (MCD) spectroscopy in paramagnetic transition metal and f-element organometallic chemistry. Dalton Transactions, 2021, 50, 416-428.	3.3	10
75	Experimental and computational studies of the mechanism of iron-catalysed C–H activation/functionalisation with allyl electrophiles. Chemical Science, 2021, 12, 9398-9407.	7.4	10
76	Air-Stable Iron-Based Precatalysts for Suzuki–Miyaura Cross-Coupling Reactions between Alkyl Halides and Aryl Boronic Esters. Organic Process Research and Development, 2021, 25, 2461-2472.	2.7	10
77	Side-on coordination of diphosphorus to a mononuclear iron center. Science, 2022, 375, 1393-1397.	12.6	9
78	Crystal structure of a third polymorph of tris(acetylacetonato-κ ² <i>O</i> , <i>O</i> ′)iron(III). Acta Crystallographica Section E: Crystallographic Communications, 2015, 71, m228-m229.	0.5	8
79	Geometric Structure Determination of N694C Lipoxygenase: A Comparative Near-Edge X-Ray Absorption Spectroscopy and Extended X-Ray Absorption Fine Structure Study. Inorganic Chemistry, 2008, 47, 11543-11550.	4.0	7
80	Syntheses and characterizations of iron complexes of bulky <i>o</i> -phenylenediamide ligand. Dalton Transactions, 2020, 49, 12287-12297.	3.3	5
81	Anion-induced disproportionation of Th(<scp>iii</scp>) complexes to form Th(<scp>ii</scp>) and Th(<scp>iv</scp>) products. Chemical Communications, 2022, 58, 5289-5291.	4.1	5
82	Homoleptic Aryl Complexes of Uranium (IV). Angewandte Chemie, 2019, 131, 10372-10376.	2.0	4
83	TMEDA in Iron atalyzed Hydromagnesiation: Formation of Iron(II)â€Alkyl Species for Controlled Reduction to Alkeneâ€Stabilized Iron(0). Angewandte Chemie, 2020, 132, 17218-17224.	2.0	4
84	Dilithium Amides as a Modular Bis-Anionic Ligand Platform for Iron-Catalyzed Cross-Coupling. Organic Letters, 2021, 23, 5958-5963.	4.6	4
85	A TMEDA–Iron Adduct Reaction Manifold in Ironâ€Catalyzed C(sp ²)â^'C(sp ³) Cross oupling Reactions. Angewandte Chemie - International Edition, 2022, 61, .	13.8	4
86	Direct observation of ICT cations at the HTL/transparent semiconductor interface. Organic Electronics, 2014, 15, 3761-3765.	2.6	2
87	Synthesis and characterization of a sterically encumbered homoleptic tetraalkyliron(III) ferrate complex. Polyhedron, 2019, 158, 91-96.	2.2	2
88	Forged in iron. Nature Reviews Chemistry, 2021, 5, 223-224.	30.2	2
89	NHC Effects on Reduction Dynamics in Iron atalyzed Organic Transformations**. Chemistry - A European Journal, 2021, 27, 13651-13658.	3.3	2
90	Near-infrared <i>C</i> -term MCD spectroscopy of octahedral uranium(<scp>v</scp>) complexes. Dalton Transactions, 2021, 50, 5483-5492.	3.3	2

#	Article	IF	CITATIONS
91	Intermediates and mechanism in iron-catalyzed C–H methylation with trimethylaluminum. Chemical Communications, 2021, 57, 12784-12787.	4.1	2
92	Resident holes and electrons at organic/conductor and organic/organic interfaces: An electron paramagnetic resonance investigation. Organic Electronics, 2016, 37, 379-385.	2.6	1
93	Isolation and Characterization of a Homoleptic Tetramethylcobalt(III) Distorted Square-Planar Complex. Organometallics, 2019, 38, 3486-3489.	2.3	1
94	The Exceptional Diversity of Homoleptic Uranium–Methyl Complexes. Angewandte Chemie, 2020, 132, 13688-13692.	2.0	1
95	Characterization Methods for Paramagnetic Organometallic Complexes. , 2022, , 135-175.		1
96	C H Activation/Functionalization With Earth Abundant 3d Transition Metals. , 2021, , 260-310.		1
97	Crystal structure of bromidopentakis(tetrahydrofuran-ΰ <i>O</i>)magnesium bis[1,2-bis(diphenylphosphanyl)benzene-ΰ ² <i>P</i> , <i>P</i> @€2]cobaltate(â~1) tetrahydrofuran disolvate. Acta Crystallographica Section E: Crystallographic Communications, 2019, 75, 304-307.	0.5	1
98	Crystal structures of two new six-coordinate iron(III) complexes with 1,2-bis(diphenylphosphane) ligands. Acta Crystallographica Section E: Crystallographic Communications, 2018, 74, 803-807.	0.5	0
99	Recent Advances in Synthesis, Characterization and Reactivities of Iron-Alkyl and Iron-Aryl Complexes. , 2021, , .		Ο
100	A TMEDAâ€Iron Adduct Reaction Manifold in Ironâ€Catalyzed C(sp2)â€C(sp3) Crossâ€Coupling Reactions. Angewandte Chemie, 0, , .	2.0	0